



## Accumulation of phosphatidylcholine on gut mucosal surface is not dominated by electrostatic interactions



Agatha Korytowski<sup>a</sup>, Wasim Abuillan<sup>a</sup>, Federico Amadei<sup>a</sup>, Ali Makky<sup>a,1</sup>, Andrea Gumiero<sup>b</sup>, Irmgard Sinning<sup>b</sup>, Annika Gauss<sup>c</sup>, Wolfgang Stremmel<sup>c,\*</sup>, Motomu Tanaka<sup>a,d,\*\*</sup>

<sup>a</sup> Physical Chemistry of Biosystems, Institute of Physical Chemistry, Heidelberg University, D69120 Heidelberg, Germany

<sup>b</sup> Heidelberg University Biochemistry Center (BZH), D69120 Heidelberg, Germany

<sup>c</sup> Department of Internal Medicine IV, University Clinics of Heidelberg, D69120 Heidelberg, Germany

<sup>d</sup> Institute for Integrated Cell-Material Science (WPI iCeMS), Kyoto University, 606-8501 Kyoto, Japan

### ARTICLE INFO

#### Article history:

Received 18 August 2016

Received in revised form 19 January 2017

Accepted 11 February 2017

Available online 15 February 2017

#### Keywords:

Ulcerative colitis

Mucin

Lipid-protein interaction

Light scattering

Electrostatics

Isothermal titration calorimetry

### ABSTRACT

The accumulation of phosphatidylcholine (PC) in the intestinal mucus layer is crucial for the protection of colon epithelia from the bacterial attack. It has been reported that the depletion of PC is a distinct feature of ulcerative colitis. Here we addressed the question how PC interacts with its binding proteins, the mucins, which may establish the hydrophobic barrier against colonic microbiota. In the first step, the interactions of dioleoylphosphatidylcholine (DOPC) with two mucin preparations from porcine stomach, have been studied using dynamic light scattering, zeta potential measurement, and Langmuir isotherms, suggesting that mucin binds to the surface of DOPC vesicles. The enthalpy of mucin-PC interaction could be determined by isothermal titration calorimetry. The high affinity to PC found for both mucin types seems reasonable, as they mainly consist of mucin 2, a major constituent of the flowing mucus. Moreover, by the systematic variation of net charges, we concluded that the zwitterionic DOPC has the strongest binding affinity that cannot be explained within the electrostatic interactions between charged molecules.

© 2017 Elsevier B.V. All rights reserved.

### 1. Introduction

The colonic lumen contains a large amount of bacteria that amounts to one trillion per gram of stool, colonic epithelial cells are protected from attack by the huge bacterial load by a mucus layer [1]. The protective mucus scaffolds consist of a family of highly glycosylated proteins, mucins [2]. The main intestinal secretory protein, mucin 2, is secreted by goblet cells [3] but enterocytes express transmembrane mucins 3, 12, 13 and 17 in the vicinity of apical tight junctions [2,4]. A mounting evidence suggested that the protective function of mucus against the bacterial invasion is established by phospholipids [5]. Phosphatidylcholine (PC) and lyso-phosphatidylcholine (lyso-PC) share more than 90% of the phospholipids within the intestinal mucus [6], suggesting that PC/lyso-PC are either selectively transported or bound to this

compartment. Since goblet cells secreting mucin do not store phospholipids, a separate PC secretion route is postulated. A recent study unraveled that the selective transport of PC/lyso-PC is mediated via paracellular transport through tight junction to the apical side [7].

There have been several reports suggesting that the depletion of phospholipid coating and thus the disruption of mucosal barrier has been suggested as underlying cause of disease, such as ulcerative colitis [8]. For example, the colon intestine surface of rats orally treated with detergents exhibited a decrease in both water contact angles and barrier capability against dextran sodium sulfate [5]. Actually, in human ulcerative colitis, PC and lyso-PC molecules in the intestinal mucus are reduced by 70% [6,8]. From the very simple viewpoint of interfacial free energy, it is plausible that the mucus layer and wet lumen or biofilms should be interfaced by the formation of a lipid bilayer, while the mucosal layer in contact with the dry (ambient) atmosphere should be stabilized by a lipid monolayer (Scheme 1).

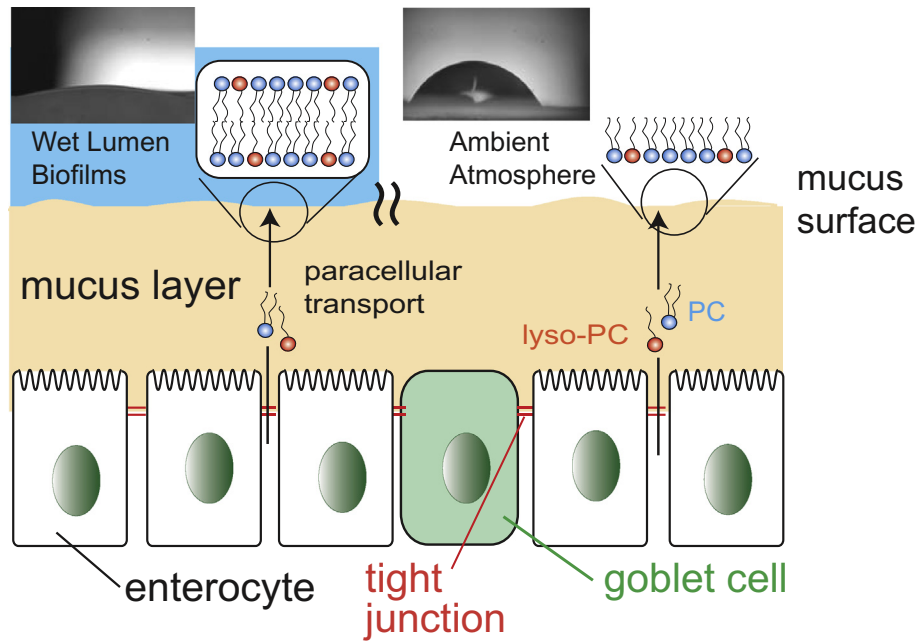
In this study, we shed light on the mechanism how PC/lyso-PC molecules are selectively accumulated on mucus surfaces, where a barrier against colonic microbiota is generated. To address this question, we studied the interactions of lipids and two mucin preparations from the flowing mucus, whose main constituent is mucin 2. The systematic

\* Corresponding author.

\*\* Correspondence to: M. Tanaka, Physical Chemistry of Biosystems, Institute of Physical Chemistry, Heidelberg University, D69120 Heidelberg, Germany.

E-mail addresses: [Wolfgang.Stremmel@med.uni-heidelberg.de](mailto:Wolfgang.Stremmel@med.uni-heidelberg.de) (W. Stremmel), [tanaka@uni-heidelberg.de](mailto:tanaka@uni-heidelberg.de) (M. Tanaka).

<sup>1</sup> Present address: CNRS UMR 8612, Institut Galien Paris-Sud, Faculté de Pharmacie, 5 rue J.B. Clément, 92296 Châtenay-Malabry, France.



**Scheme 1.** Transport of phospholipid through the tight junction in colon epithelia (goblet cells, enterocytes) and accumulation to the mucus layer surface. Establishment of the protection layer by amphiphilic lipids can be evidenced by simple contact angle measurements. The explant from rat colon epithelial tissue pre-treated with water (left) showed a very low contact angle ( $\theta < 20^\circ$ ), suggesting the protection by a lipid bilayer in contact with wet lumen or biofilms. On the other hand, the same tissue exposed to an ambient atmosphere (right) exhibited a much higher contact angle ( $\theta \sim 70^\circ$ ), implying the formation of a lipid monolayer.

combination of several experimental techniques unraveled the molecular parameters that dictate the significance of lipid-mucin interactions.

## 2. Experimental section

### 2.1. Materials

Deionized water from a Milli-Q device (Millipore, Molsheim, France) was used throughout this study. In this study we used two types of mucin products from porcine stomach (Sigma-Aldrich, Munich, Germany): mucin type II (MS2378) is a crude preparation of mucin, while mucin type III (M1778) is a partially purified preparation following the previously reported protocol [9]. It should be noted that the nomenclature, following that of the manufacturer, has no correlation with mucin 2 and mucin 3. As the unidentified impurities would influence some of the results, we confirmed the reproducibility of the results by repeating experiments using samples from two different batches. Chloroform solutions of lipids were purchased from Avanti Polar Lipids (AL, USA) throughout this study. As the lipid model, we used four lipids that possess identical hydrocarbon chains but different head groups: DOPC (1,2-dioleoyl-*sn*-glycero-3-phosphocholine) and DOPE (1,2-dioleoyl-*sn*-glycero-3-phosphoethanolamine) as zwitterionic ( $\pm$ ), DOTAP (1,2-dioleoyl-3-trimethylammonium-propane) as cationic (+), and DOPG (1,2-dioleoyl-*sn*-glycero-3-phospho-(1'-*rac*-glycerol)) as anionic (−) lipids. Unless stated otherwise, all other chemicals were purchased either from Sigma-Aldrich (Munich, Germany) or Carl Roth (Karlsruhe, Germany), and were used without further purification. As the buffer, HEPES buffered saline containing 150 mM NaCl, 10 mM HEPES (4-(2-hydroxyethyl)-1-piperazineethanesulfonic acid), and 0.1 mM ethylenediaminetetraacetic acid (EDTA) adjusted to pH 7.4 was used throughout this study.

The following static light scattering, dynamic light scattering and zeta potential measurements were performed in HEPES buffer using a Malvern Zetasizer Nano ZS (Malvern Instruments Ltd., UK) equipped with a He-Ne laser with a wavelength of 632.8 nm with a backscattering geometry at a constant scattering angle of  $173^\circ$ . Values for viscosity, refractive index and dielectric constant of HEPES buffer were chosen from

the manufacturer's database (viscosity 1.0021 cP, refractive index 1.330 and relative dielectric constant 80.4). A refractive index of 1.45 was used for mucin proteins.

### 2.2. Static Light Scattering (SLS)

A 800  $\mu\text{L}$  portion of mucin solution was filled in a square glass cuvette, and the scattering intensity from different concentrations was measured. The SLS measurements were repeated 6 times each consisting of 10 runs with a single run duration of 10 s. A refractive index increment of 0.1 mL/g was used for mucin solution.

### 2.3. Surface activity

Critical aggregation concentration ( $c^*$ ) of mucin was calculated from the surface tension of 60  $\mu\text{L}$  suspensions (concentrations: 20  $\mu\text{g}/\text{mL}$ –10 mg/mL) using a Kibron Micro TroughX (Kibron Inc., Espoo, Finland). Each data point corresponds to a mean value of at least three independent measurements.

### 2.4. Dynamic Light Scattering (DLS)

A 100  $\mu\text{L}$  portion of mucin solution (10 mg/mL) was added to a 300  $\mu\text{L}$  portion of vesicle suspension (1 mM), prepared by extrusion through a polycarbonate membrane with a pore size of 100 nm (Avestin, Mannheim, Germany). As the apparent molecular weight of mucin obtained from SLS does not correspond to the native one due to the preparation protocols (Footnote: information from the manufacturer), the weight concentration of mucin was kept constant to compare mucin type II and mucin type III. DLS experiments were carried out at  $25^\circ\text{C}$ . DLS measurements on pure mucin were repeated 3 times each consisting of 100 to 500 runs with a single run duration of 30 s while that on mucin and vesicle suspensions were repeated more than 5 times with a single run duration of 60 s. The raw data were analyzed as distribution by intensity with Igor PRO (WaveMetrics, Portland, USA) software using a log-normal function  $f(x,K) = K_0 + K_1 * \exp - [\ln(x/K_2)/K_3]^2$  yielding the position of the maximum from  $K_2$  and the full width at half maximum (FWHM)

from  $K_3$ , where  $K_0$  is the offset and  $K_1$  is the weight. To monitor the change in the multiple population including small protein particles, we also monitored the size distribution normalized by number, too.

### 2.5. Zeta potential

After a short equilibration time (2 min) at 20 °C, the sample in a folded capillary cell was subjected to the measurement under a constant voltage (150 mV). Zeta potential measurements were repeated 3 times each consisting of 100 to 500 runs with a single run duration of 30 s. The zeta potential  $\zeta$  was analyzed according to the Smoluchowski equation [10] using the software provided by the manufacturer:  $\zeta = \mu\eta\varepsilon^{-1}$ , where  $\mu$  is experimentally determined electrophoretic mobility,  $\eta$  viscosity and  $\varepsilon$  dielectric constant.

### 2.6. Langmuir isotherms

Pressure-area isotherms were recorded with a Langmuir film balance (KSV, Helsinki). The lipid stock solution (1 mg/mL in  $\text{CHCl}_3$ ) was spread on the buffer subphase. After the evaporation of the solvent (10 min), the mucin solution (0.5 mg/mL) was injected under the barrier. After 1 h, the film was compressed at a constant speed of 1–10 Å<sup>2</sup> per molecule per minute.

### 2.7. Isothermal titration calorimetry

The thermodynamic parameters of lipid-mucin interactions were measured at 25 °C using a MicroCal VP-ITC (Malvern, United Kingdom) after the calibration with 0.1 mM  $\text{CaCl}_2$  (syringe) and 1 mM EDTA (sample cell). The concentrations of lipid suspensions and mucin solutions were 50 μM and 10 mg/mL, respectively. As concentrated solutions of mucin were highly viscous, vesicle suspensions were injected into the sample cell filled with mucin. The data were analyzed with the software provided by the manufacturer.

## 3. Results and discussion

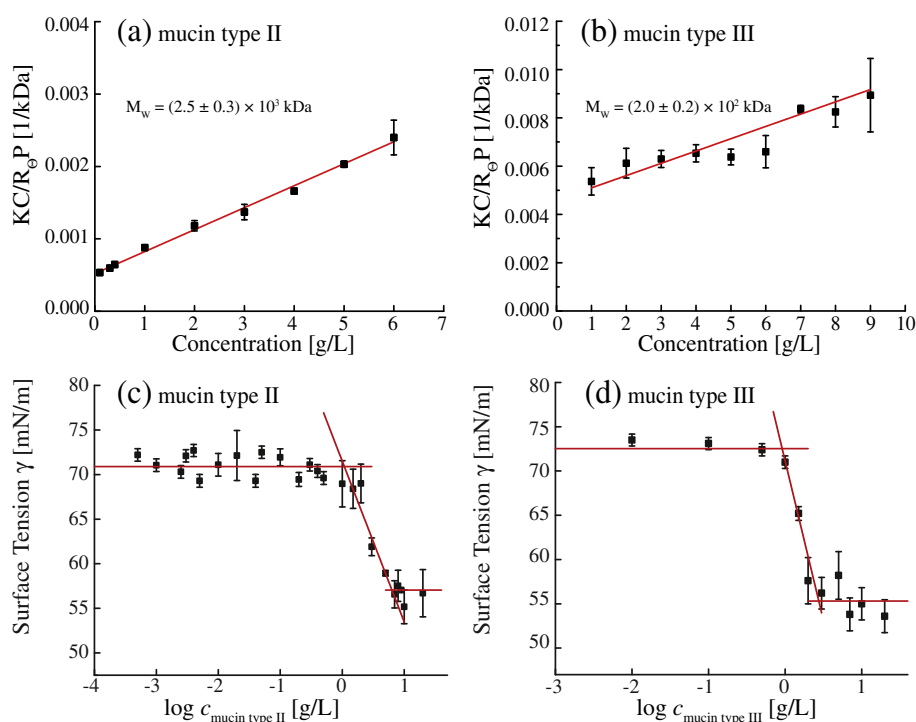
### 3.1. Basic characterization of mucin in solution

Fig. 1a and b represents the so-called Zimm plot:

$$\frac{KC}{R(\theta)} = \frac{1}{M_w P(\theta)} + 2A_2 C$$

where  $K$  is constant,  $C$  concentration of the scattering particle,  $R(\theta)$  form factor (Rayleigh ratio),  $P(\theta)$  structure factor, and  $A_2$  second virial coefficient. As the slope of a Zimm plot and thus the second virial coefficient reflects the relative significance of particle-particle vs. particle-solvent interactions, the positive slopes obtained from both mucin preparations imply that the solutions of both mucin preparations are stable. The apparent molecular weight of mucin type II determined by SLS was found to be more than 10 times larger than that of mucin type III:  $MW_{\text{mucinII}} = (2.5 \pm 0.3) \times 10^3$  kDa and  $MW_{\text{mucinIII}} = (2.0 \pm 0.2) \times 10^2$  kDa. The apparently larger  $M_w$  obtained for mucin type II seems plausible because mucin III is partially purified from mucin type II [9]. Although these values are of fractionated portion of mucin and thus may not be the molecular weights of native mucin, both molecular weight values lie within the range reported for mucin extracted from porcine stomach mucosa,  $2 \times 10^2$ – $1.6 \times 10^7$  kDa [11].

In the next step, we compared the surface activities of mucin type II and mucin type III. Fig. 1c and d represents surface tensions of mucin solution plotted as a function of weight concentration. This enables one to determine the critical aggregate concentrations  $c^*$  of mucin type II and mucin type III,  $c^*_{\text{mucinII}} = 7$  mg/mL and  $c^*_{\text{mucinIII}} = 2$  mg/mL, respectively. Interestingly, the  $c^*$  values we obtained here seem comparable to the overlapping concentrations determined by the rheological characterization of porcine stomach mucin, 3 mg/mL [11]. This apparent agreement qualitatively seems plausible if one considers highly hydrophilic nature of mucin in general. Namely, mucin molecules become surface active when they start interacting with each other.



**Fig. 1.** Determination of the molecular weight of (a) mucin type II and (b) mucin type III from SLS analysis (Zimm plot). Surface tensions of (c) mucin type II and (d) mucin type III measured at different concentrations.

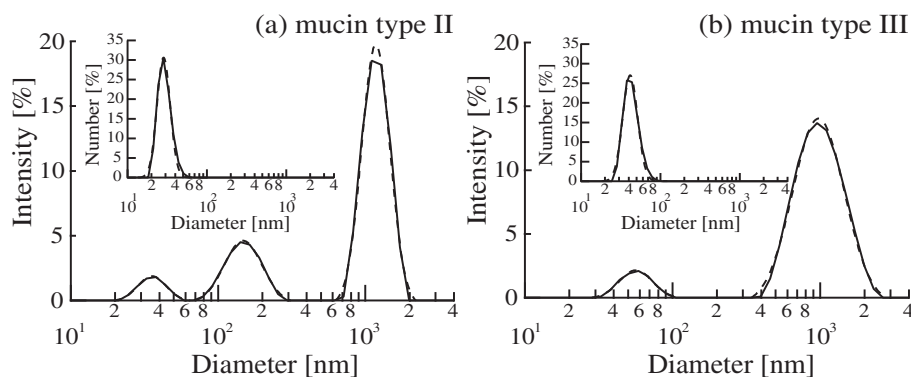


**Fig. 2.** Size distributions of (a) mucin type II and (b) mucin type III normalized by dynamic light scattering intensity (black). The broken lines are the fitting results with multiple log-normal functions. For the comparison, the corresponding size distributions normalized by number are presented in insets.

**Fig. 2** represents the intensity size distributions of (a) mucin type II and (b) mucin type III. Note that the experiments were performed at the concentration of 10 mg/mL, which is above the  $c^*$  of both mucin. Though the multiple peaks observed by the intensity-normalized size distributions (main panels) suggested the formation of  $\mu\text{m}$ -order aggregates, the size distributions normalized by number (insets) suggest that the vast majority (>99%) of mucin type II and mucin type III proteins have diameter of  $\Phi_{\text{mucinII}} = 28 \pm 7$  nm and  $\Phi_{\text{mucinIII}} = 46 \pm 11$  nm, respectively. As naturally occurring mucin 2 contains cysteine-rich domains. Since cysteine-rich domains in mucin could cross-link mucin into viscoelastic gels, we performed DLS of mucin in the presence of 1,4-dithiothreitol (DTT) that reduces disulfide bonds. As presented in Supplemental Fig. 1, we found no notable change in the DLS signals even in the presence of 1 M DTT, suggesting that the molecular weight determination was not biased by the cross-linking mediated by disulfide bridges. Previously, Silva et al., measured the dynamic light scattering of mucin type III at pH 3.0 in the presence and absence of chitosan [12] and claimed much larger “apparent particle diameters” (about 260 and 1300 nm). However it is very difficult to compare these data because they assumed much larger molecular weight (29 MDa) without SLS measurements and the pH condition (pH 3.0) of their experiments is far too acidic compared to the pH in large intestine (pH 5.5–7.0). In addition, we performed the DLS measurements at pH 5.5, confirming that the size distributions of mucin type II and mucin type III are comparable to those measured at pH 7.4 (Supplemental Fig. S2).

### 3.2. Mucin-phosphocholine (PC) interactions

The interactions between mucin and phospholipids were firstly examined by monitoring changes in the hydrodynamic radius after mixing DOPC vesicles and mucin solutions. **Fig. 3** represents the DLS signals of pure DOPC vesicles (black solid), pure mucin (black broken), mixtures at  $t = 10$  min (green) and 60 min (red). For both mucin type II and mucin type III, characteristic mucin peaks disappear after the mixing.

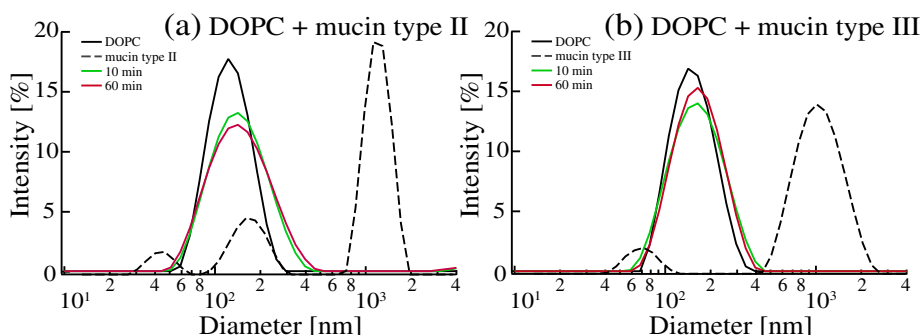


**Fig. 3.** Intensity-normalized size distributions of DOPC vesicles after incubation with (a) mucin type II and (b) mucin type III determined by dynamic light scattering.

The characteristic peak for DOPC vesicles exhibited a distinct increase in both the average diameter and FWHM. In case of mucin type II (panel a), the shift of the peak position from 124 nm ( $t = 0$  min, pure DOPC) to 142 nm ( $t = 60$  min) was accompanied by a broadening of the peak width FWHM from 98 nm ( $t = 0$  min, pure DOPC) to 165 nm ( $t = 60$  min). In case of mucin type III (panel b), we also observed a shift of the peak position from 149 nm ( $t = 0$  min) to 165 nm ( $t = 60$  min) as well as the increase in FWHM from 124 nm ( $t = 0$  min) to 161 nm ( $t = 60$  min). More detailed kinetic data are presented in Supplemental Fig. S3. Although the significance of interactions between mucin type II and mucin type III cannot be compared conclusively, the relative changes in  $\Phi$  and FWHM suggest that interaction of DOPC with mucin type II (a larger Mw) is stronger than DOPC-mucin type III interaction.

The increase in peak position as well as the broadening of size distribution compared to pure DOPC (black) suggests that the surface of DOPC vesicles is coated by “mucin layer”. This hypothesis is also supported by the disappearance of the characteristic mucin peaks for both mucin type II and mucin type III. Additionally, we observed that the incubation of mucin solutions and lyso-PC micelles ( $\Phi = 3\text{--}4$  nm) [13] resulted in the decrease of the characteristic lyso-PC peak from 10 to 3.5% suggesting the adsorption of lyso-PC micelles on the mucin surface (Supplemental Fig. S4). To verify the presence of mucin layers on vesicle surfaces, we measured the zeta potentials of DOPC vesicles in the absence and presence of mucin. **Fig. 4** represents the zeta potentials of pure DOPC (open circles, prior to mixing defined as  $t = 0$  min), mucin solutions (open squares,  $t = 0$  min), and DOPC-mucin mixture recorded over time (solid squares). DOPC vesicle suspensions showed the zeta potentials of around  $\zeta_{\text{DOPC}} = -2$  mV, and both mucin type II and mucin type III had very similar values;  $\zeta_{\text{mucinII}} \approx \zeta_{\text{mucinIII}} = -7$  mV independent from the concentration. Upon mixing, we found that the zeta potentials of DOPC vesicles converges to the level near mucin  $\zeta_{\text{after}} = -7$  to  $-6$  mV already after 10 min. Therefore, the combination of DLS and zeta potential measurements confirmed that the surface of DOPC

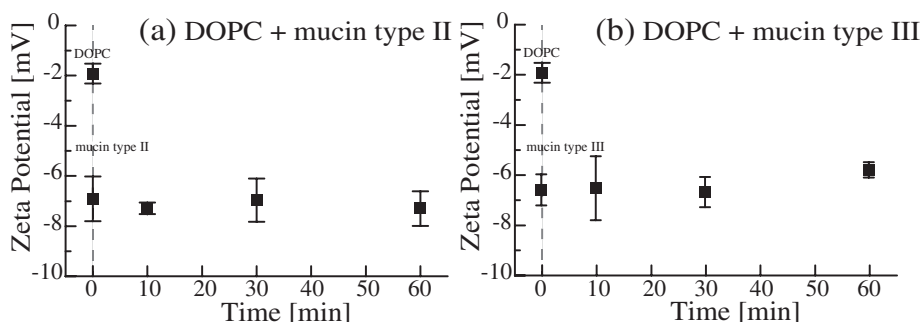


Fig. 4. Changes in zeta potentials recorded after mixing DOPC vesicles and (a) mucin type II and (b) mucin type III.

vesicles is coated by mucin. The fact that the zeta potential of DOPC-mucin type II suspensions and that of DOPC-mucin type III suspensions are very similar seems reasonable as these two preparations have similar sialic acid contents (information from the manufacturer).

To further verify the binding of mucin to the surface of PC membranes, we measured the pressure-area isotherms of DOPC monolayers at the air/water interface (Fig. 5, solid). In the presence of both mucin type II (broken) and mucin type III (dashed), the onset of pressure increase was observed at much larger area per molecule  $A \approx 140 \text{ \AA}^2$  compared to pure DOPC. The monolayers in the presence of mucin occupied distinctly larger areas compared to the pure DOPC monolayer until the surface pressure reached  $\pi \approx 30 \text{ mN/m}$ , suggesting that absorption of mucin bound to DOPC to the air/water interface. In other words, at a constant area per molecule, the presence of both mucin preparations caused the distinct increase in surface pressure, as reported for the interactions between cationic peptides and negatively charged membranes driven by the electrostatics [14–19]. In fact, the lateral compression modulus  $\kappa = A(\partial\pi/\partial A)_T$  of DOPC monolayer was clearly smaller in the presence of mucin in comparison to the pure DOPC monolayer (Fig. 5, inset). It should be noted that the injection of mucin to the subphase after the compression of a DOPC monolayer did not cause an increase in surface pressure (data not shown), which can be attributed to the slow diffusion of mucin in the subphase. Moreover, the DOPC monolayer structure remained intact after the addition of mucin as determined by X-ray reflectivity indicating that mucin molecules do not penetrate into DOPC membrane (Supplemental Fig. S5).

Thermodynamics of mucin-DOPC interactions was further investigated by isothermal titration calorimetry experiments. Fig. 6 represents the calorimetric titration pattern recorded over time by the titration of DOPC (50  $\mu\text{M}$ ) with mucin type III solutions (10 mg/mL). The

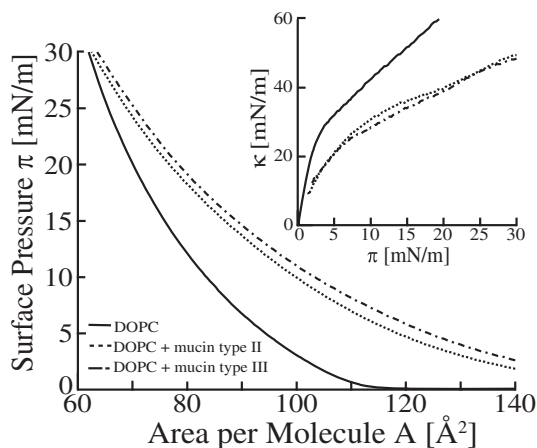


Fig. 5. Pressure area isotherms of DOPC monolayers in the absence (solid) and presence of mucin type II (broken) and mucin type III (dashed). The compression modulus  $\kappa = A(\partial\pi/\partial A)_T$  calculated from the isotherms are presented in the inset.

corresponding heat of reactions plotted as a function of molar ratio is displayed in the inset, yielding the reaction enthalpy of  $\Delta H^0 = (-1.4 \pm 0.2) \times 10^4 \text{ cal/mol}$  and the binding constant of  $K_0 = (1.4 \pm 0.9) \times 10^7 \text{ M}^{-1}$ . Throughout the experiments, we often observed the baseline shift (data not shown), which indicates mucin sticks to the vesicle wall. Based on this reason, the experiments with mucin type II solution were practically very difficult. From two successful experiments, we found that the reaction enthalpy  $\Delta H^0 = (-6.0 \pm 1.0) \times 10^4 \text{ cal/mol}$  is more than 4 times larger than that of mucin type III, and  $K_0 = (2.4 \pm 0.7) \times 10^7 \text{ M}^{-1}$  is also distinctly higher. This finding is in qualitative agreement with the relative significance of interaction suggested by DLS results, suggesting the interaction of DOPC with mucin type II is stronger than DOPC-mucin type III interaction (Fig. 3). Since both mucin preparations are predominantly mucin 2, the strong DOPC-mucin interactions suggested for both preparations seems to explain the selective transport of PC and lyso-PC molecules to the surface of intestinal mucosal layers [6].

### 3.3. Influence of electrostatics

The fact that mucin proteins are negatively charged proteins with a lot of sialic acid residues naturally draws the next question: How strongly do lipid-mucin interactions depend on electrostatics? To further assess the effect of electrostatics, we performed the ITC experiments of DOPC vesicles incorporating 20 mol% of lipids that possess same dioleoyl hydrocarbon chains but different head groups (Scheme 2): DOTAP (+) and DOPG (-). First, the vesicles containing negatively charged DOPG showed the weakest interaction with mucin type III,  $\Delta H_{\text{DOPG-mucinIII}} = (-4.0 \pm 0.2) \times 10^3 \text{ cal/mol}$  and  $K_{\text{DOPG-mucinIII}} = (4.5 \pm 1.1) \times 10^6 \text{ M}^{-1}$ . This finding can be attributed to the electrostatic repulsion between negatively charged mucin and negatively charged DOPG. More interestingly, the interaction between mucin type III and vesicles incorporating positively charged DOTAP was only slightly stronger

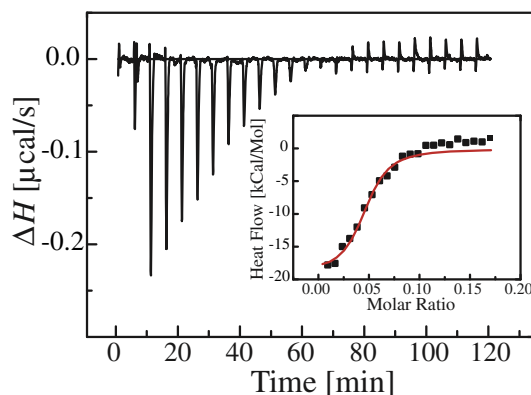
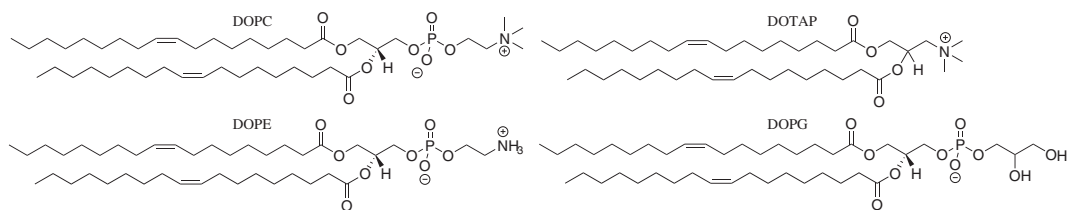


Fig. 6. Calorimetric pattern recorded over time by the titration of DOPC with mucin type III solutions and the corresponding heat of reactions (inset).



**Scheme 2.** Chemical structures of lipids used in this study.

than DOPG but much weaker than DOPC;  $\Delta H_{\text{DOTAP-mucinIII}} = (-7.9 \pm 0.9) \times 10^3$  cal/mol and  $K_{\text{DOTAP-mucinIII}} = (6.5 \pm 3.1) \times 10^6$  M<sup>-1</sup>. This finding indicates the doping of 20 mol% of cationic DOTAP even resulted in the decrease in the reaction enthalpy by almost 40%. In addition, grazing incidence X-ray fluorescence experiments showed no enrichment of K<sup>+</sup> and Cl<sup>-</sup> ions at the DOPC monolayer after the addition of mucin type III (1 mg/mL), excluding the effect of electrostatics on mucin-DOPC interaction (Supplemental Fig. S6).

To verify the potential influence of electrostatics on mucin-lipid interactions, we also measured Langmuir isotherms of pure DOPG and DOTAP, and investigated the influence of mucin type II and mucin type III (Fig. 7). As clearly indicated in the main panels and insets of the figure, the presence of both mucin proteins did not cause any remarkable change in the global shape of isotherms as well as the compression moduli  $\kappa$ , suggesting that both mucin proteins do not interact with pure DOPG (-) or DOTAP (+).

### 3.4. Biological relevance, possible mechanisms

As previously reported, the mucosal coating of gut epithelia is protected against the aggressive attack by bacteria by the phospholipid layer, and more than 90% of phospholipids in intestinal mucus are identified as PC and lyso-PC [6]. In this study, both DLS results and Langmuir isotherms unanimously suggest that DOPC interacts strongly with both mucin preparations, containing mucin 2 predominantly. Does this finding make any sense from the biological viewpoint? In gut intestines, mucin 2 is a major constituent of the intestinal mucus layer that continuously flows on the epithelial surfaces. In contrast, other family members, like mucins 3, 12, 13, and 17, are transmembrane proteins expressed on the apical side of gut epithelial cells. From this context, the stronger interactions of PC with preparations containing mucin 2 seem to cause the accumulation of PC to the mucosal surfaces after the paracellular transport, instead of the deposition of the membrane-anchored mucus layer on epithelial cells. Comparing lipids with different head groups, we found that zwitterionic PC has the strongest affinity.

What is the dominant molecular interaction that dictates lipid-mucin interactions? Our experimental results clearly excluded the electrostatic interactions. Not only negatively charged DOPG (-), but also

positively charged DOTAP (+) resulted in a drastic decrease in the binding strength. DOPC vesicles doped with 20 mol% of DOPG exhibited a decrease in the reaction enthalpy by a factor of more than 3 compared to pure DOPC vesicles. More interestingly, only 20 mol% positively charged DOTAP already caused a 40% decrease in the reaction enthalpy. The former can be attributed to the electrostatic repulsion between negatively charged mucin and DOPG, but the latter cannot. The fact that positively charged DOTAP is less interactive with mucin strongly suggests that role of electrostatics is not dominant. Indeed, the ITC experiments of another zwitterionic lipid DOPE ( $\pm$ ) suggested an even stronger interaction with mucin type III compared to DOPC,  $\Delta H_{\text{DOPE-mucinIII}} = (-8.8 \pm 0.7) \times 10^4$  cal/mol. Although this may be attributed to the difference in spatial accessibility of proteins between bulky PC and more compact PE head groups [20], it should be noted that pure DOPE suspensions cannot sustain vesicular shapes, resulting in the enhancement of the curvature-induced lipid-protein interaction [21].

Recently, an increasing number of studies suggested the unique physical properties of molecules with zwitterionic moieties. For example, hydration, conformation, and anti-fouling of synthetic polymer brushes with zwitterionic side chains do not follow the classical Hofmeister series [22–23]. This finding suggests the interdigitation of the neighboring zwitterionic side chains [22]. In fact, dendrimers possessing choline phosphate functions are shown to glue the membranes [24]. Further investigations, such as the determination of element-specific density profiles [25–27] or nonlinear optical spectroscopy of water in the proximity of interfaces [28–29], would shed light on the interfacial interaction between intestinal mucosa and zwitterionic lipids.

## 4. Conclusions

Intestinal mucus protects gut epithelia from the aggressive attack of bacteria by the surface layer composed of phospholipids, whose major constituent is phosphatidylcholine (PC). To understand the molecular level mechanism of PC accumulation in intestinal mucus after the selective paracellular transfer, we systematically investigated interactions of lipids and mucin. As the mammalian mucus model, we used mucin type II and mucin type III from porcine stomach. Although these are crude fractions after enzymatic digestions, the Zimm plot analysis of static light scattering results suggested relatively uniform molecular weights

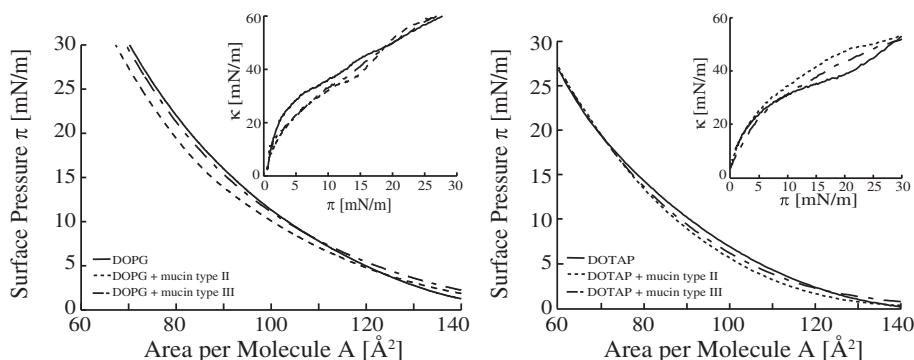


**Fig. 7.** Pressure-area isotherms (main panels) and compression moduli of (a) DOPG and (b) DOTAP monolayers in the presence and absence of mucin type II and mucin type III.

for both mucin type II ( $M_{w, \text{mucinII}} \sim 2.5$  MDa) and mucin type III ( $M_{w, \text{mucinIII}} \sim 0.2$  MDa). Dynamic light scattering experiments implied that interaction with mucin caused an increase in the hydrodynamic radius and a broadening of the width of size distribution of DOPC vesicles. The binding and coating of mucin on DOPC membrane surfaces were further supported by zeta potential measurements as well as by the global shape and the lateral compressibility obtained from Langmuir isotherms. Thermodynamics of mucin-DOPC interaction was studied by using isothermal titration calorimetry, yielding the  $\Delta H^0 \sim -60$  kcal/mol by taking the molecular weight of 0.2 MDa determined by SLS.

The influence of electrostatics was investigated by the systematic variation of the net charge of head groups. DOPC vesicles doped with 20 mol% of DOPG (–) showed the reaction enthalpy of  $\Delta H^0_{\text{DOPG-mucinIII}} = -4$  kcal/mol, which can be explained as the electrostatic repulsion between negatively charged mucin and DOPG (–). However, the incorporation of 20 mol% of DOTAP (+) also resulted in a lower reaction enthalpy than pure DOPC,  $\Delta H^0_{\text{DOTAP-mucinIII}} \sim -8$  kcal/mol. A clear decrease in the reaction heat caused by 20 mol% doping of DOTAP,  $\Delta H^0_{\text{DOTAP-mucinIII}} - \Delta H^0_{\text{DOPC}} \sim 6$  kcal/mol, confirmed that the electrostatic interaction does not play any dominant role in lipid-mucin interactions. In fact, another zwitterionic lipid with a more compact ethanolamine head group, DOPE ( $\pm$ ), even exhibited a higher mucin affinity compared to DOPC. Thus, our experimental findings provide with the first quantitative evidence that the binding affinity of PC and mucin, especially to mucin type II secreted by goblet cells, is the underlying mechanism of the accumulation of PC in intestine mucosa, which cannot be explained merely by classical electrostatic interactions.

## Acknowledgements

M.T. thanks O.G. Mouritsen and P.K.J. Kinnunen for insightful comments. This work was supported by EU FP7 BIBAFOODS No. 606713 (M.T. and F.A.) and Phospholipid Research Center No. 120300 (M.T. and W.S.). M.T. and I.S. are investigators of the Cluster of Excellence “Cell Networks”. iCeMS is supported by World Premier International Research Center Initiative (WPI), MEXT, Japan.

## Appendix A. Supplementary data

Supplementary data to this article can be found online at <http://dx.doi.org/10.1016/j.bbmem.2017.02.008>.

## References

- [1] C.L. Maynard, C.O. Elson, R.D. Hatton, C.T. Weaver, Reciprocal interactions of the intestinal microbiota and immune system, *Nature* 489 (2012) 231–241.
- [2] M.E.V. Johansson, H. Sjövall, G.C. Hansson, The gastrointestinal mucus system in health and disease, *Nat. Rev. Gastroenterol. Hepatol.* 10 (2013) 352–361.
- [3] Y.S. Kim, S.B. Ho, Intestinal Goblet Cells and Mucins in Health and Disease: Recent Insights and Progress, 12, 2010 319–330.
- [4] T. Pelaseyed, J.H. Bergström, J.K. Gustafsson, A. Ermund, G.M.H. Birchenough, A. Schütte, S. van der Post, F. Svensson, A.M. Rodríguez-Piñero, E.E.L. Nyström, C. Wising, M.E.V. Johansson, G.C. Hansson, The mucus and mucins of the goblet cells and enterocytes provide the first defense line of the gastrointestinal tract and interact with the immune system, *Immunol. Rev.* 260 (2014) 8–20.
- [5] A. Lugea, A. Salas, J. Casalot, F. Guarner, J.-R. Malagelada, Surface hydrophobicity of the rat colonic mucosa is a defensive barrier against macromolecules and toxins, *Gut* 46 (2000) 515–521.
- [6] R. Ehehalt, J. Wagenblast, G. Erben, W.D. Lehmann, U. Hinz, U. Merle, W. Stremmel, Phosphatidylcholine and lysophosphatidylcholine in intestinal mucus of ulcerative colitis patients. A quantitative approach by nano-electrospray-tandem mass spectrometry, *Scand. J. Gastroenterol.* 39 (2004) 737–742.
- [7] W. Stremmel, S. Staffer, H. Gan-Schreier, A. Wannhoff, M. Bach, A. Gauss, Phosphatidylcholine passes through lateral tight junctions for paracellular transport to the apical side of the polarized intestinal tumor cell-line CaCo2, *Biochim. Biophys. Acta Mol. Cell Biol. Lipids* 1861 (2016) 1161–1169.
- [8] A. Braun, I. Treede, D. Gotthardt, A. Tietje, A. Zahn, R. Ruhwald, U. Schoenfeld, T. Welsch, P. Kienle, G. Erben, W.-D. Lehmann, J. Fuellekrug, W. Stremmel, R. Ehehalt, Alterations of phospholipid concentration and species composition of the intestinal mucus barrier in ulcerative colitis: a clue to pathogenesis, *Inflamm. Bowel Dis.* 15 (2009) 1705–1720.
- [9] D. Glenister, K.E. Salamon, K. Smith, D. Bighton, C. Keevil, Enhanced growth of complex communities of dental plaque bacteria in mucin-limited continuous culture, *Microb. Ecol. Health Dis.* 1 (1988) 31–38.
- [10] A. Sze, D. Erickson, L. Ren, D. Li, Zeta-potential measurement using the Smoluchowski equation and the slope of the current-time relationship in electroosmotic flow, *J. Colloid Interface Sci.* 261 (2003) 402–410.
- [11] T.A. Waigh, A. Papagiannopoulos, A. Voice, R. Bansil, A.P. Unwin, C.D. Dewhurst, B. Turner, N. Afdhal, Entanglement coupling in porcine stomach mucin, *Langmuir* 18 (2002) 7188–7195.
- [12] C.A. Silva, T.M. Nobre, F.J. Pavinatto, O.N. Oliveira, Interaction of chitosan and mucin in a biomembrane model environment, *J. Colloid Interface Sci.* 376 (2012) 289–295.
- [13] G. Vitiello, D. Ciccarelli, O. Ortona, G. D’Errico, Microstructural characterization of lysophosphatidylcholine micellar aggregates: the structural basis for their use as biomembrane mimics, *J. Colloid Interface Sci.* 336 (2009) 827–833.
- [14] M.R. Yeaman, N.Y. Yount, Mechanisms of antimicrobial peptide action and resistance, *Pharmacol. Rev.* 55 (2003) 27–55.
- [15] L. Zhang, A. Rozek, R.E.W. Hancock, Interaction of cationic antimicrobial peptides with model membranes, *J. Biol. Chem.* 276 (2001) 35714–35722.
- [16] S.E. Blondelle, K. Lohner, M.-I. Aguilar, Lipid-induced conformation and lipid-binding properties of cytolytic and antimicrobial peptides: determination and biological specificity, *Biochim. Biophys. Acta Biomembr.* 1462 (1999) 89–108.
- [17] R.G. Oliveira, E. Schneck, B. Quinn, O. Konovalov, T. Gill, C. Hanna, D.A. Pink, M. Tanaka, Physical mechanism of bacterial survival revealed by combined grazing-incidence X-ray scattering and Monte Carlo simulation, *C. R. 12* (2009) 209–217.
- [18] H. Zhao, R. Sood, A. Jutila, S. Bose, G. Fimland, J. Nissen-Meyer, P.K. Kinnunen, Interaction of the antimicrobial peptide piperocin with model membranes: implications for a novel mechanism of action, *Biochim. Biophys. Acta Biomembr.* 1758 (2006) 1461–1474.
- [19] C.D. Fjell, J.A. Hiss, R.E. Hancock, G. Schneider, Designing antimicrobial peptides: form follows function, *Nat. Rev. Drug Discov.* 11 (2012) 37–51.
- [20] J.N. Israelachvili, D.J. Mitchell, B.W. Ninham, Theory of self-assembly of hydrocarbon amphiphiles into micelles and bilayers, *J. Chem. Soc. Faraday Trans. 2* (1976) 1525–1568.
- [21] K. Iwamoto, T. Hayakawa, M. Murate, A. Makino, K. Ito, T. Fujisawa, T. Kobayashi, Curvature-dependent recognition of ethanolamine phospholipids by duramycin and cinnamycin, *Biophys. J.* 93 (2007) 1608–1619.
- [22] T. Wang, X. Wang, Y. Long, G. Liu, G. Zhang, Ion-specific conformational behavior of polyzwitterionic brushes: exploiting it for protein adsorption/desorption control, *Langmuir* 29 (2013) 6588–6596.
- [23] M. Kobayashi, Y. Terayama, M. Kikuchi, A. Takahara, Chain dimensions and surface characterization of superhydrophilic polymer brushes with zwitterion side groups, *Soft Matter* 9 (2013) 5138–5148.
- [24] X. Yu, Z. Liu, J. Janzen, I. Chafeeva, S. Horte, W. Chen, R.K. Kainthan, J.N. Kizhakkedathu, D.E. Brooks, Polyvalent choline phosphate as a universal biomembrane adhesive, *Nat. Mater.* 11 (2012) 468–476.
- [25] E. Schneck, T. Schubert, O.V. Konovalov, B.E. Quinn, T. Gutsmann, K. Brandenburg, R.G. Oliveira, D.A. Pink, M. Tanaka, Quantitative determination of ion distributions in bacterial lipopolysaccharide membranes by grazing-incidence X-ray fluorescence, *Proc. Natl. Acad. Sci. U. S. A.* 107 (2010) 9147–9151.
- [26] W. Abouillan, A. Vorobiev, A. Hartel, N.G. Jones, M. Engstler, M. Tanaka, Quantitative determination of the lateral density and intermolecular correlation between proteins anchored on the membrane surfaces using grazing incidence small-angle X-ray scattering and grazing incidence X-ray fluorescence, *J. Chem. Phys.* 137 (2012) 204907–204908.
- [27] A. Körner, W. Abouillan, C. Deichmann, F.F. Rossetti, A. Köhler, O.V. Konovalov, D. Wedlich, M. Tanaka, Quantitative determination of lateral concentration and depth profile of histidine-tagged recombinant proteins probed by grazing incidence X-ray fluorescence, *J. Phys. Chem. B* 117 (2013) 5002–5008.
- [28] Y. Zhang, S. Furry, D.E. Bergbreiter, P.S. Cremer, Specific ion effects on the water solubility of macromolecules: PNIPAM and the Hofmeister series, *J. Am. Chem. Soc.* 127 (2005) 14505–14510.
- [29] X. Chen, T. Yang, S. Kataoka, P.S. Cremer, Specific ion effects on interfacial water structure near macromolecules, *J. Am. Chem. Soc.* 129 (2007) 12272–12279.